

Sense Shimming (Sensh); a fast approach for determining field inhomogeneities using coil sensitivity information

D. N. Splitthoff¹, and M. Zaitsev¹

¹Dept. of Diagnostic Radiology, Medical Physics, University Hospital Freiburg, Freiburg, BW, Germany

Introduction: Although modern MR scanners produce highly homogeneous fields, this feature is often more than counterbalanced by the increased susceptibility artifacts at higher field strengths (>=3T). Therefore the scanners are equipped with a large set of so-called shim coils which can be used for reversing the effects of the inhomogeneities. The process of finding the right parameters for the coil adjustment is termed "shimming". Different shimming methods have been proposed, depending on the accuracy, i.e. order ([1]), ranging from acquisitions of projections along the three axes ([2-4]) for the linear case, or along selected diagonals ([5]) for additional second orders, to full 3D field maps. We will here present a proof of principle of a new method for determining the coefficients of field inhomogeneities which benefits from the increased trend not only to higher field strengths, but to a higher number of receiver coils as well. The technique can be seen as a special case of the SENSE parallel imaging method ([6]) and will therefore be introduced here as SENS (SENSe SHimming).

Methods: Modern routine receiver coils consist of arrays of 12 elements or more; head-arrays with 192 elements have been presented. As has been shown by Pruessmann et al. in ([6]), the spatially varying sensitivity of the individual elements can be used as additional spatial encoding information. This allows for reducing the amount of needed frequency and phase encoding steps while maintaining the maximum k-space values; thus the acquisition time can be shortened by a so-called reduction factor R. The resulting fold-overs can be resolved by reconstructing separate images for the coil elements and using the previously measured sensitivities for unfolding.

The method to be presented here is a special case of this setup: we abstain completely from using traditional frequency and phase encoding, thus obtaining a fold-over of all pixel into one, i.e. a FID. Knowing the sensitivity information and spin density, basis functions corresponding to fields generated by shim coils can be fitted as will be shown in the following:

The signal received in channel n without encoding at time t can be described as follows:

$$\Psi_n(t) = \int_{dV} \rho(\vec{r}) s_n(\vec{r}) e^{i\omega(\vec{r})t} = \int_{dV} \rho(\vec{r}) s_n(\vec{r}) e^{i\omega(\vec{r})t_0} e^{i\omega(\vec{r})\Delta t} = \int_{dV} \rho_n'(\vec{r}, t_0) e^{i\omega(\vec{r})\Delta t} \quad (1)$$

where $\rho_n'(\vec{r}, t_0) = \rho(\vec{r}) s_n(\vec{r}) e^{i\omega(\vec{r})t_0}$; $\rho(\vec{r})$ and $s_n(\vec{r})$ are the real spin density and the complex sensitivity for coil n, respectively. $\omega(\vec{r})$ describes the field inhomogeneities at point \vec{r} and $\Delta t = t - t_0$. For small inhomogeneities and/or short Δt the exponential function in equation (1) can be approximated to $e^{i\omega(\vec{r})\Delta t} \approx 1 + i\omega(\vec{r})\Delta t$ and the full equation reads

$$\Psi_n(t) = \int_{dV} \rho_n'(\vec{r}) + i\Delta t \int_{dV} \rho_n'(\vec{r}) \omega(\vec{r}) \quad (2)$$

Knowing $\rho_n'(\vec{r}, t_0)$ for a given t_0 would thus allow for estimating the FID signal at time $t_0 + \Delta t$. Fortunately $\rho_n'(\vec{r}, t_0)$ can be interpreted as the reconstructed image for coil n for a GRE sequence with $TE = t_0$; no true sensitivity map acquisition and calculation is therefore needed. The alternative is to set $t_0 = 0$, i.e. to acquire the FID signal early enough after the excitation to still fulfil the approximation of a small phase change. This implies use of non-selective excitation pulses, and receiver coils with a sufficiently high number of elements distributed in 3D. Calculating the derivative of equation (2) yields

$$-i(\Psi_n(t_0 + \Delta t) - \Psi_n(t_0)) / \Delta t = T_n = \int_{dV} \rho_n'(\vec{r}) \omega(\vec{r}) \quad (3)$$

For discrete image slices this can be rewritten with matrices and solved in a least square sense: $u = [C^T C]^{-1} C^T v$, with $C = PB$, B being the matrix consisting of basis functions, P a matrix with the measured image data and v a vector with the T_n ; u is a vector containing the coefficients. It is obvious, that the approximation of the exponential function in equation (2) will be equal to unity for $\Delta t = T_{dwell}$, with the dwell time T_{dwell} in the order of microseconds and for small inhomogeneities; in this case the derivative in equation (3) is dominated by noise. Δt has therefore to be chosen with care, in order to obtain sufficiently high signal in equation (3) and still fulfil the approximation condition. In the discrete case $t = f\Delta t$, with f being a scaling factor.

Results & Discussion: For demonstration purposes a 12 channel head array with a circular alignment of elements was used; the following simulations and experiments are therefore restricted to the in-plane case. In the simulations, using the presented framework, P was set to data obtained with the mentioned coil from a FLASH measurement with $TE = 3ms$. Setting $\Delta t = T_{dwell} = 0.0078ms$ and simulating a gradient of $4\mu T/m$, Figure 1 shows the importance of choosing a good temporal scaling factor f in the presence of noise (f ranges from 30 to 230, SNR from $20 \cdot 10^6$ to $3 \cdot 10^5$). In a next step phantom experiments were carried out with the mentioned FLASH sequence and deactivated frequency and phase encoding gradients. The shim settings were purposely altered (in $1\mu T/m$ steps: $X = -3..3$ and $Y = -3..3$); in order to account for the necessary scaling factor, the derivative was calculated over ± 110 FID points taken from one line. The results are shown in Figure 2.

Keeping in mind, that this is only a proof of principle and that results should improve with an increasing number of coil elements, it is to be expected, that results can still be improved significantly.

References: [1] Hillenbrand et al., AMR 29, 39-64, 2005; [2] Ward et al., MRM 48, 771-780, 2002; [3] van der Kouwe et al., MRM 56, 1019-1032, 2006; [4] Splitthoff et al; Proc. ISMRM 15, Berlin, 2007; [5] Gruetter et al., MRM 43, 319-323, 2000; [6] Pruessmann et al. MRM 42, 952-962, 1999.

Acknowledgements: This work was supported in equal parts by the German Federal Ministry of Education and Research, grant #01EQ0605, and the German Research Foundation, grant #422/2-1.

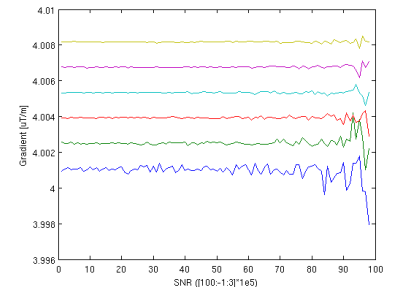


Figure 1: The six lines represent from bottom to top scaling factors from 30 to 230, with a simulated gradient of $4\mu T/m$. Shown is the respectively calculated gradient in dependency of SNR (decreasing from left to right, from $20 \cdot 10^6$ to $3 \cdot 10^5$).

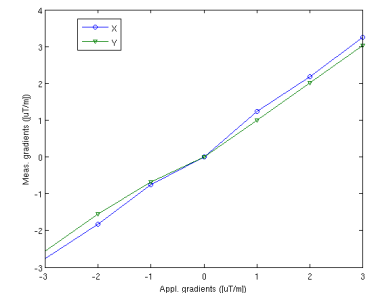


Figure 2: Applied versus measured gradients for a phantom experiment; a high linearity is given in both axes.